Effects of Structural Motion on Separation and Separation Control: An Integrated Investigation using Numerical Simulations, Theory, Wind-Tunnel and Free-Flight Experiments

Hermann F. Fasel[1], Shirzad Hosseinverdi[1], Jesse Little[1], and Andreas Gross[2]
[1]*Aerospace & Mechanical Engineering Department, University of Arizona, Tucson, AZ 85718*
[2]*Mechanical & Aerospace Engineering Dept., New Mexico State Univ., Las Cruces, NM 88003*
Email Contact: faselh@email.arizona.edu

Abstract: A combined investigative approach which employs high-fidelity numerical simulations, wind & water-tunnel and free-flight experiments is taken to investigate the fundamental flow physics of separation and separation control for wing sections undergoing temporal motions. Detailed investigations of the underlying unsteady flow physics have been carried out for the X-56A airfoil at nominal angles of attack of 10 and 12 degrees for Re = 200k. The reduced frequency of the structural motion is k=0.7 and the plunging amplitude is 3.2% and 4.8% of the chord length. For 10deg AoA, the agreement between the measurements, simulations, and Theodorsen's theory is good even though the instantaneous angles of attack during the airfoil oscillations are outside the linear $C_L - AoA$ regime and extend into the region associated with static stall. As the angle of attack is increased to 12deg, the flow over the suction surface of the wing begins to intermittently separate and Theodorsen's theory fails. Experiments and simulations show strong qualitative agreement and both capture "bursting" of the laminar separation bubble near the leading edge of the airfoil. Furthermore, highly resolved Direct Numerical Simulations (DNS) were performed in order to investigate the hydrodynamic instability mechanisms and transition to turbulence in swept laminar separation bubbles.

Keywords: Unsteady boundary-layer separation, laminar-turbulent transition, wing motion, swept wings.

Introduction

For most of the published research addressing separation for wing sections the effect of wing motion on the fluid dynamics is neglected. In the near-stall and/or full-stall regime some degree of wing movement is always present. With the current trend towards aerodynamically more efficient flexible high-aspect-ratio composite wings, this effect will become even more relevant in the future. Therefore, the consideration of the wing motion is crucially required for the successful implementation of flow control strategies in future advanced military and civilian aircraft. Our combined research approach addresses this critical issue by employing CFD simulations, wind-tunnel and free-flight experiments for investigating the fundamental flow physics of separation and its control for wing sections that are undergoing temporal (oscillatory, or impulse) motions resulting from fluid-structure interactions, atmospheric unsteadiness, engine vibrations, etc. By directly describing the wing movement in the investigations, the proposed research sets itself apart from existing fluid-structure interaction research. The focus here is not on the fluid-structure interaction per se, but rather on the effect of the airfoil motion on the fundamental flow physics of separation and its control. The parameter space for this (w.r.t., Reynolds number, pitching and/or plunging amplitude and frequency) is very different from flapping wing research and is therefore highly relevant for larger UAVs and/or full-size aircraft. The objective of the current research is to provide a fundamental physics-based understanding of how unsteady wing motion affects separation and its control for lifting surfaces. This improved understanding will ultimately lead to guidelines for the design of novel flexible composite wings with reduced fatigue loads or tailored elastic properties, such that the structural motion can be exploited for flow control.

Despite the large amount of research carried out for laminar-turbulent transition in laminar separation bubbles (LSBs) and considerable advances made in the understanding of the relevant mechanisms, our knowledge regarding swept separation bubbles is quite limited. To contribute towards a better understanding of the highly complex flow physics of LSBs in three-dimensional boundary layers, highly resolved 3D DNS are carried for a LSBs developing on a flat plate generated by a strong favorable-to-adverse pressure gradient for different sweep angles.

Methodology

To investigate the interaction of structural motion and separation, with support from the Air Force Office of Scientific Research (AFOSR) a collaborative research program was initiated at the University of Arizona (UA) and New Mexico State University (NMSU). Free-flight experiments are being carried out at the University of Arizona (UA) to map out the relevant parameter space (amplitudes, frequencies and Reynolds numbers) which will then be used for the CFD simulations and wind-tunnel experiments. Two different dynamically scaled models of the X-56A have been designed for scientific flight experiments. The X-56A, also known as the MUTT flight demonstrator, is a product of the AFRL-led Multi-Utility Aeroelastic Demonstration (MAD) program as shown in Fig. 1a. The airplane was designed and constructed by Lockheed Martin's Skunk Works. At the University of

Arizona, a 1:3 dynamically scaled model of the X-56A has been designed and built (see Fig. 1b) and its flight readiness was demonstrated. The aircraft is currently waiting to be instrumented for scientific flight tests.

The X-56A airfoil is investigated in the new low free-stream turbulence subsonic wind tunnel at the UA. A plunging apparatus was designed and built for subjecting wing sections to plunging motions up to 20Hz (see Fig. 2a). It consists of an electric motor and a system of linkages that convert the rotational motion of the motor to a linear motion of the model (Mertens et al.[1]). A 1ft chord X-56A airfoil (AR=3) was instrumented with pressure taps near midspan and mounted vertically in the wind tunnel. The model is connected to a custom plunging apparatus that operates near the eigen-frequency of the flight-test model. In parallel, Implicit Large Eddy Simulations (ILES) are performed at NMSU. This multi-tiered approach allows for the cross-validation of the different investigative tools (free-flight & wind-tunnel experiments, simulations) and thus increases chances for breakthroughs in this difficult field of research. A research Computational Fluid Dynamics (CFD) code that solves the compressible Navier-Stokes equations in curvilinear coordinates was employed for the present wing section simulations.[2] Rigid grid movement is accomplished through a time-dependent coordinate transformation.[3] The convective terms of the Navier-Stokes equations were discretized with a ninth-order-accurate van Leer scheme[4] and a fourth-order-accurate discretization was employed for the viscous terms. An implicit second-order-accurate Adams-Moulton method was used for time integration. An O-grid with high orthogonality and smoothness was generated with a Poisson grid generator (Fig. 2b). The number of cells in the circumferential, wall-normal, and spanwise direction is 400x100x32. The grid extent in the radial and spanwise direction is 10c and 0.2c, respectively.

A 3-D incompressible Navier-Stokes code using high-order accurate finite-difference approximations was employed for the DNS of LSBs. This code was developed in our CFD Laboratory and validated for numerous investigations of boundary-layer transition and LSBs (Meitz & Fasel[5], Hosseinverdi et al.[6], Balzer & Fasel[7], Hosseinverdi & Fasel[8]). For details see Meitz & Fasel.[5] The simulation setup is guided by water-tunnel experiments that are being carried out at the Hydrodynamics Laboratory of the University of Arizona. The setup of the simulations for the swept LSB simulations is illustrated in Fig. 2c (separation is generated on a flat plate as in the experiments).

Results

The wing section experiments and simulations for Re=200k are discussed first. The phase-averaged lift coefficient for α=10deg, k=0.7, and h=0.032 is presented in Fig. 3a. A slight phase shift is observed between simulation and Theodorsen's theory. Compared to the experiment, the simulation data is almost perfectly harmonic and lacks the slight experimental lift increase near φ=270deg which is a consequence of flow separation. For α=12deg, k=0.7, and h=0.048 both experiment and simulation deviate from theory (Fig. 3b) mostly with respect to the phase. Near φ=300deg the drag coefficient becomes very large indicating a significant amount of flow separation. For 270deg<φ<45deg the lift coefficient for the simulation is lower than for the experiment. During the upstroke, for φ=75deg the drag coefficient attains a minimum indicating flow reattachment. Instantaneous flow visualizations (Fig. 4a) reveal a progressing trailing edge separation during the downstroke (90deg<φ<270deg) that persists into the first half of the upstroke (270deg<φ<360deg). Both experiment and simulation capture the laminar separation bubble at the leading edge, however, a more aggressive trailing edge separation is observed in the experiment (see Fig. 4b).

Building on our previous research for unswept laminar separation bubbles[6,7,8], highly resolved DNS were employed to investigate the effect of crossflow on LSBs. From a technical application point of view, an elevated free-stream turbulence intensity (FSTI) is often responsible for laminar-turbulent transition and has thus to be considered when investigating laminar-to-turbulent transition in LSBs. In the simulations, isotropic grid turbulence was introduced at the inflow boundary (see Hosseinverdi et al.[6] and Balzer & Fasel[7] for details). The chordwise variation of the time- and spanwise-averaged skin-friction coefficient for different sweep angles are plotted in Fig. 5 for both the natural quiet scenario (FSTI=0) and for a scenario with an elevated FSTI of 0.1%. For FSTI=0, preliminary results show that the mean separation length is essentially independent of the sweep angle. Major differences for the unswept and swept flow become visible when a FSTI of 0.1% is introduced in the simulations. The mean separation length is reduced by 66.1% for 45deg sweep compared to the zero FST case. The reductions are 48% and 37.3% for the 30deg swept and unswept case, respectively. Iso-surfaces of the λ_2-criterion[9] are shown in Fig. 6. For FSTI=0%, large spanwise coherent structures are forming because of shear layer instability. These structures are commonly called 'spanwise rollers' or Kelvin-Helmholtz vortices. For a FSTI of 0.1%, the free-stream turbulence induces low-frequency u-velocity distortions inside the laminar approach boundary-layer and disturbances with a wide range of wavelengths and frequencies (including steady disturbances) are strongly amplified.

Conclusions

Wind tunnel experiments and implicit large eddy simulations for a plunging wing section for 10 and 12deg angle of attack were found to be in good qualitative agreement. For α=10deg the lift coefficient followed Theodorsen's theory closely and the experimental and numerical data revealed minimal flow separation and a periodic thickening

and thinning of the suction side boundary layer. For 12deg angle of attack intermittent flow separation from the suction surface is observed during the downstroke and the first half of the upstroke and the lift coefficient deviates from Theodorsen's theory mainly with respect to the phase. Although quantitative agreement between experiment and simulation was achieved only over part of the plunging period, both data sets reveal a periodic bursting of the laminar leading edge bubble. The effect of wing sweep was investigated for a representative model geometry. From DNS, it was found that wing sweep considerably amplifies the effect of FST on the structure of laminar separation bubbles.

Acknowledgements

This research was funded by the Air Force Office of Scientific Research (AFOSR) (Program Manager: Dr. Douglas Smith, grant number: FA9550-14-1-0184).

References

[1]Mertens C, Pineda S, Agate M, Little J, Gross A, Fasel, H. F., 2016: Effects of Structural Motion on the Aerodynamics of the X-56A Airfoil. AIAA Paper 2016-2073.
[2]Gross, A., and Fasel, H., 2008: High-Order Accurate Numerical Method for Complex Flows. AIAA J., 46(1), pp. 204-214.
[3]Gross, A., Zhou, J., and Fasel, H.F., 2015: Numerical Simulation of Circular Cylinder and Wing Sections in Unsteady Motion. AIAA-paper AIAA-2015-3069.
[4]Gross, A., Little, J.C., and Fasel, H.F., 2016: Numerical Simulation of Wing Section Near Stall. AIAA 2016-3947.
[5]Meitz, H. & Fasel, H. F., 2000: A compact-difference scheme for the Navier-Stokes equations in vorticity-velocity formulation. J. Comp. Phys, 157, 371–403.
[6]Hosseinverdi, S., Balzer, W., and Fasel, H. F., 2012: Direct Numerical Simulations of the Effect of Free-Stream Turbulence on 'Long' Laminar Separation Bubbles. AIAA Paper 2012-2972, New Orleans, LA.
[7]Balzer, W. & Fasel, H. F., 2010: Direct numerical simulation of laminar boundary layer separation and separation control on the suction side of an airfoil at low Reynolds number conditions. AIAA Paper 2010-4866.
[8]Hosseinverdi, S and Fasel H. F., 2013: Direct Numerical Simulations of Transition to Turbulence in Two-Dimensional Laminar Separation Bubbles. AIAA Paper 2013-0264.
[9]Jeong, J. & Hussain, F., 1995: On the identification of a vortex. J. Fluid Mech, 285, 69–94.

Figures

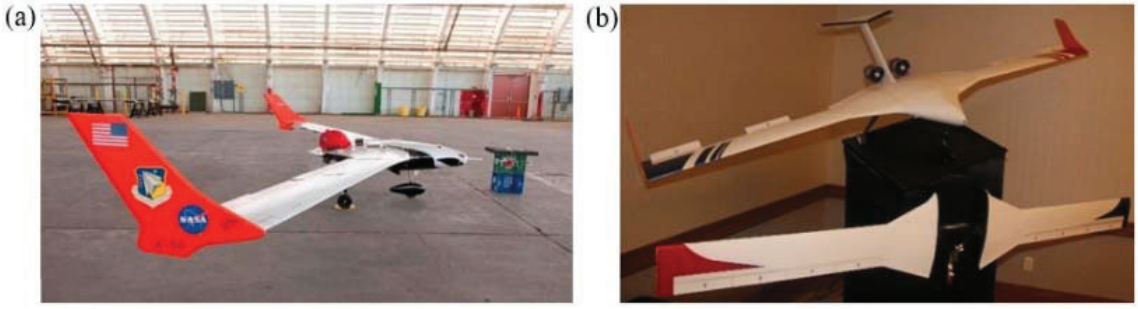

Figure 1. X-56A: a) Full size (NASA Armstrong); b) 1:3 dynamically scaled model (University of Arizona).

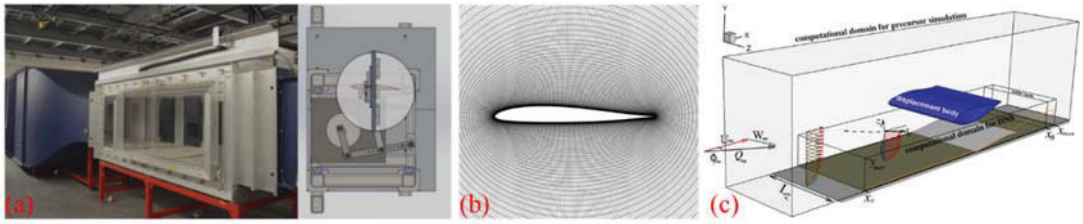

Figure 2. a) Wind tunnel and plunging mechanism, b) O-grid for wing section simulations; c) computational setup for simulating swept laminar separation bubble on flat plate.

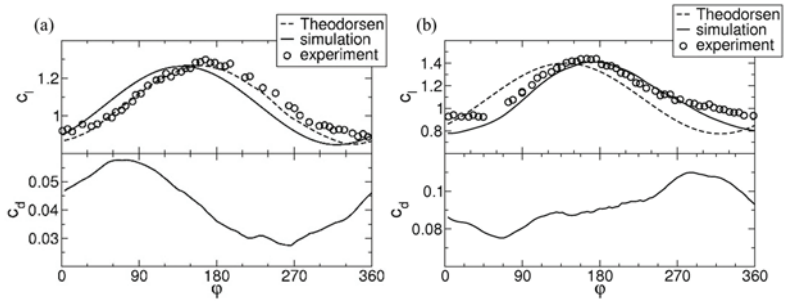

Figure 3. Lift and drag coefficient for a) α=10deg, k=0.7, h=0.032 and b) α=12deg, k=0.7, h=0.048.

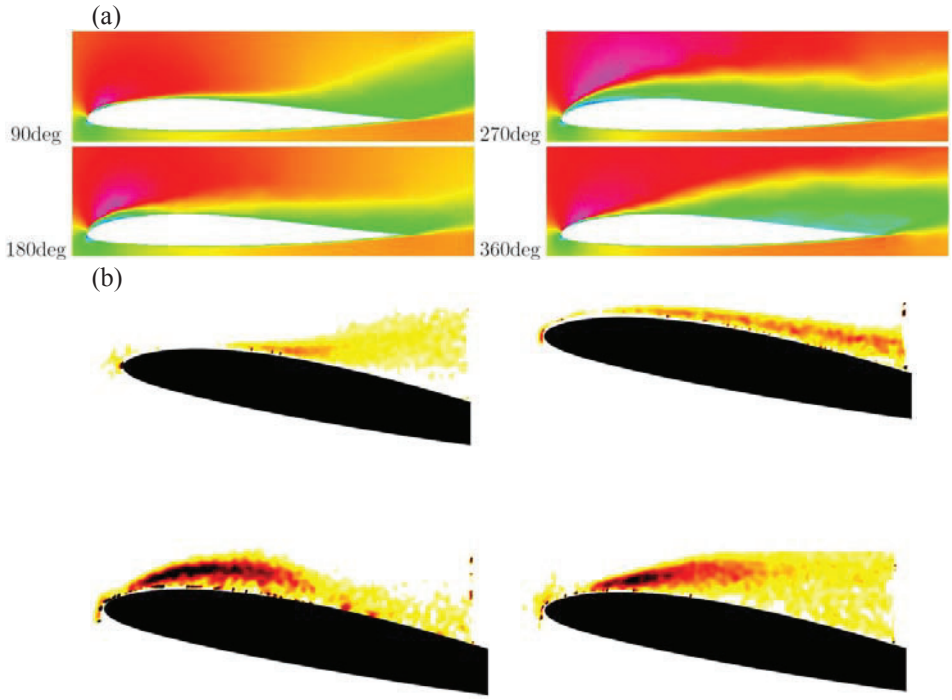

Figure 4. Flow visualiztion for α=12deg, k=0.7, h=0.048. (a) Iso-contours of u-velocity from simulations (phase and spanwise averages); (b) phase averaged vorticity (from PIV).

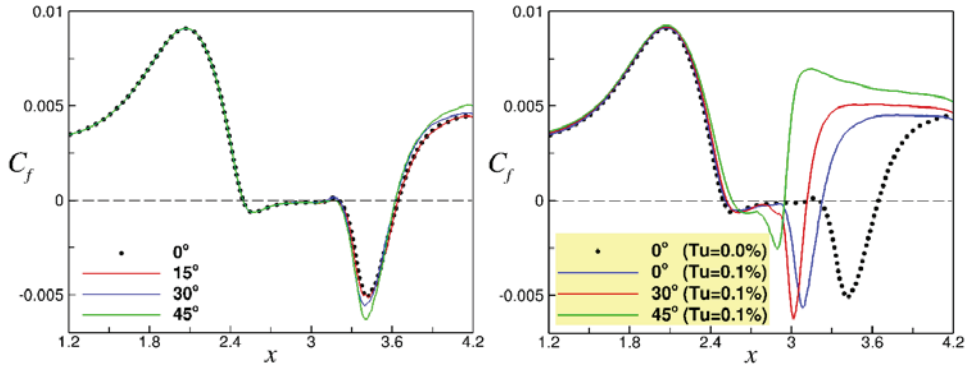

Figure 5. Time- and spanwise-averaged wall-skin friction for various sweep angles. Left: natural simulations (FSTI=0); right: FSTI=0.1%.

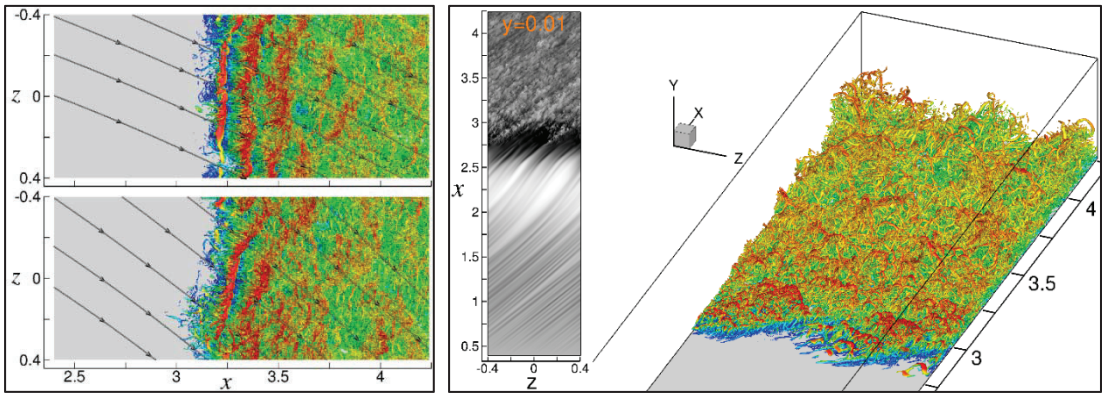

Figure 6. Instantaneous flow visualizations. Left: Top-down views of iso-surfaces of $\lambda_2 = -500$ colored by u-velocity together with inviscid streamlines for $\phi_\infty = 30^o$ (top) and $\phi_\infty = 45^o$ (bottom) for FSTI=0; right: Iso-surfaces of $\lambda_2 = -500$ colored by u-velocity together with contours of u-velocity at constant y-location for FSTI=0.1% and 45deg sweep.